

Electronic Supplementary Information (ESI) for

Small-Sized Ag Nanocrystals: High Yield Synthesis in Solid-Liquid Phase System, Growth Mechanism and Their Successful Application in Sonogashira Reaction

Min Han, Suli Liu, Xiaopeng Nie, Dan Yuan, Peipei Sun, Zhihui Dai,* and Jianchun Bao*

Jiangsu Key Laboratory of Biofunctional Materials, School of Chemistry and Materials Science, Nanjing Normal University, Nanjing 210097, P. R. China. Tel: 0086 25 85891936; E-mail: baojianchun@njnu.edu.cn; daizhihui@njnu.edu.cn

Experimental Phenomena under Temperature Programming Reaction Mode

In order to confirm the reaction is solid-liquid two phase system, the dissolving status of solid precursors and reaction process has been clearly observed during the temperature programming reaction mode. At room temperature, the solid precursor is deposited at the bottom of the reactor and the liquid layer is colorless. When the reactor is heated to 85 °C, a thin layer of black substance appears on the solid-liquid interface with a few bubbles emitting, indicating that the solid AgNO₃ is partially dissolved and reduced by DDA to form Ag crystal nuclei. With the increase of reaction temperature, the black substance is gradually transferred into the liquid layer. As the temperature is raised to 105-110 °C, some film-like substance appears on the liquid-air interface, which reflects bright blue light. Moreover, some unreacted solid precursors still deposit at the bottom of the reactor and the color of the liquid turns into green-yellow. At 130 °C, the liquid becomes opaque. Further increasing the temperature to 160 °C, the color turns to reddish brown and the bubble disappears. At 200 °C, the color becomes deep. According to those experimental phenomena, as the temperature reaches 130, 160, 200 and 260 °C, four samples are taken to examine the growth process of Ag NCs, respectively.

Magnified TEM Images of Figure 3

In order to see clearly, the **magnified TEM images for Fig. 3** are given as follow:

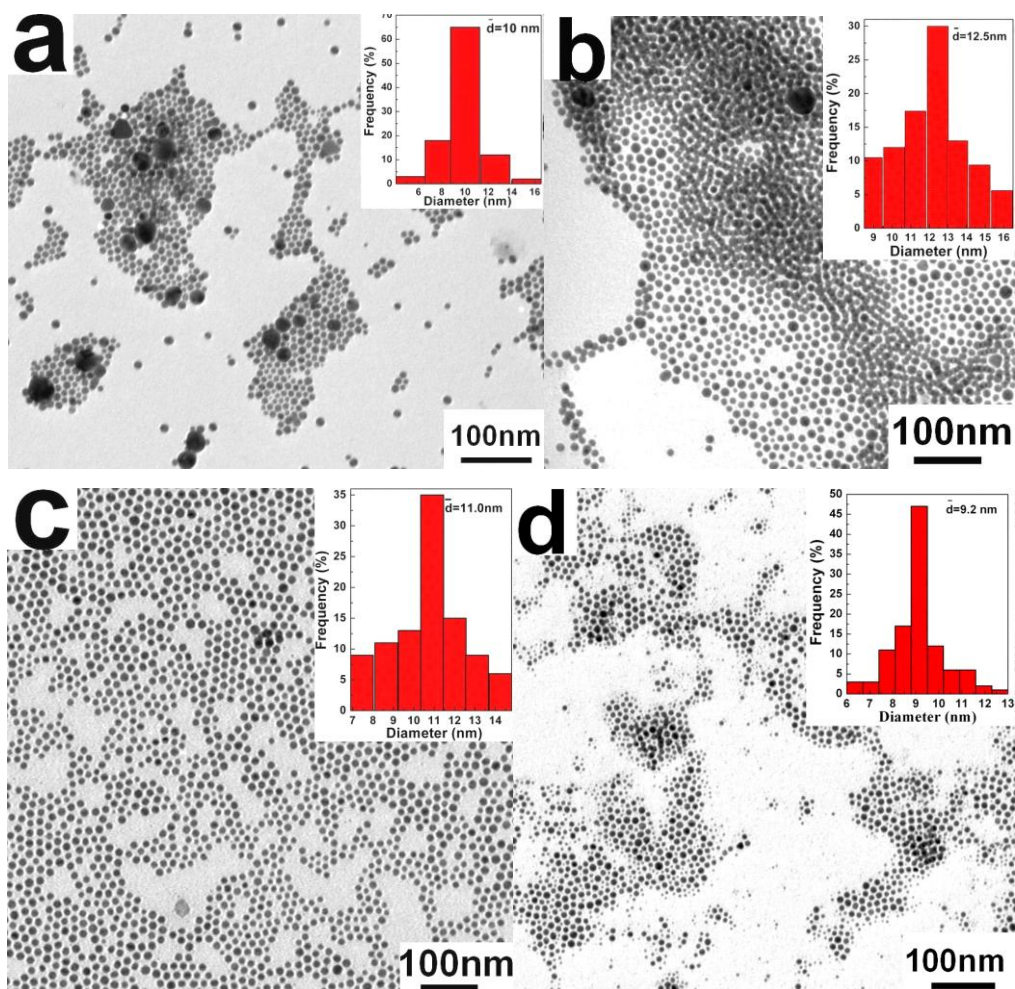


Figure 3 TEM images of the Ag NCs samples obtained at 280 °C by ripening for (a) 5 min, (b) 10 min, (c) 15 min, and (d) 25 min. (Notes: In the upper right corner of (a), only the statistical size of the small particles is listed. While in the upper right corner of (d), only the statistical size of the visible large particles is given.)

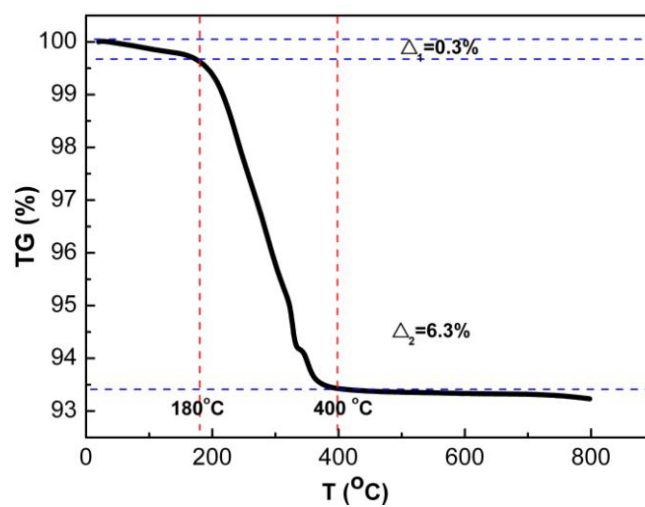


Figure S1 The thermogravimetric plot of the obtained 6 nm Ag NCs at the temperature ranging from room temperature to 800 °C under Ar gas atmosphere.

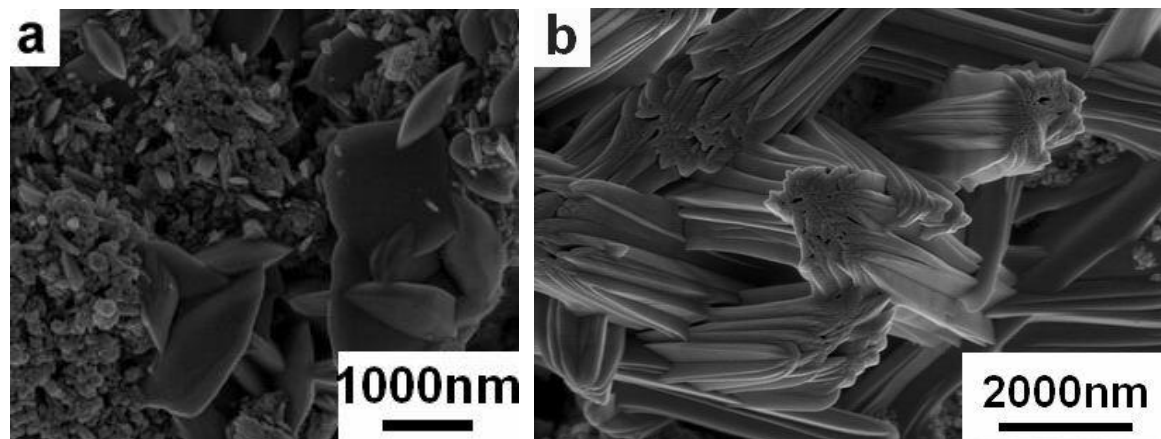


Figure S2 FE-SEM images of the Ag nanostructures synthesized at 280 °C using sodium dodecylsulfate instead of DDA. (a) Ag nanoparticles and nanoshuttles; (b) complicated 1D Ag nanoarchitectures.

Optimization of reaction conditions for Sonogashira reaction by using Ag NCs as catalyst: The coupling reaction between phenylacetylene and *p*-iodotoluene is chosen as a model reaction for optimizing the catalytic reaction conditions. The influence factors such as the solvent, the amount of Ag NCs catalyst, the amount of CuI, the amount of PPh₃, and the kind of base (to neutralize the in-situ generated strong acid during Sonogashira reaction) are carefully examined. Corresponding results are shown in **Table S1**, **Table S2**, **Table S3**, **Table S4** and **Table S5**.

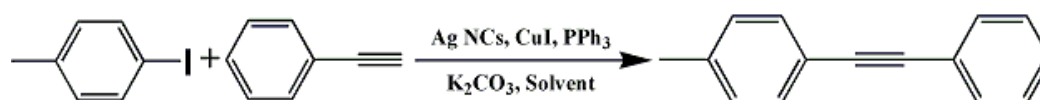


Table S1 The influence of **solvent** on the yields of the coupling reaction between phenylacetylene and *p*-iodotoluene.

Solvent	THF	NMP	DMF	acetonitrile	toluene	isopropanol
Isolated yields(%)	65	94	87	43	81	90

(Notes: Ag NCs catalyst: 5 mol%; CuI: 4 mol%; PPh₃: 5 mol%; K₂CO₃: 1.5 equiv; temperature: 80 °C; time: 2 h)

Table S2 The influence of **the amount of catalyst** (Ag NCs with the size of 6 nm) on the coupling reaction between phenylacetylene and *p*-iodotoluene

Catalyst (mol%)	10	5	3	2	0
Isolated yield (%)	96	94	55	24	trace

(Notes: CuI: 4 mol%, PPh₃: 5 mol%, K₂CO₃: 1.5 equiv, solvent: NMP, temperature: 80 °C, time: 2 h)

Table S3 The influence of **the amount of ligand (PPh₃)** on the coupling reaction between phenylacetylene and *p*-iodotoluene

PPh ₃ (mol%)	1	5	10	15
Isolated yield (%)	30	94	56	37

(Notes: Ag NCs catalyst: 5 mol%, CuI: 4 mol%, K₂CO₃: 1.5 equiv, solvent: NMP, temperature: 80 °C, time: 2 h)

Table S4 The influence of **the amount of co-catalyst (CuI)** on the coupling reaction between phenylacetylene and *p*-iodotoluene

Co-catalyst CuI (mol%)	10	5	4
Isolated yield (%)	71	83	94

(Notes: Ag NCs catalyst: 5 mol%, PPh₃: 5 mol%, K₂CO₃: 1.5 equiv, solvent: NMP, temperature: 80 °C, time: 2 h)

Table S5 The influence of **the kind of base** on the coupling reaction between phenylacetylene and *p*-iodotoluene

Base	NaOH	Na ₂ CO ₃	KOH	K ₂ CO ₃
Isolated yield (%)	47	66	trace	94

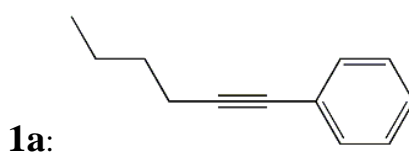
(Notes: Ag NCs catalyst: 5 mol%, CuI: 4 mol%, PPh₃: 5 mol%, base: 1.5 equiv, Solvent: NMP, temperature: 80 °C, time: 2 h.)

In Sonogashira reaction, the excess base is required to neutralize the in-situ generated acidic species. In our examined four kinds of inorganic base, the K₂CO₃ with the amount of 1.5 equiv shows the best performance. When the amount of K₂CO₃ is lower than 1.5 equiv, the neutralization process is not complete and the yield is low.

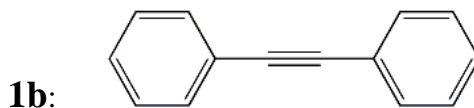
While the amount of K_2CO_3 is further increased to 2 equiv or higher than 2 equiv, the yield does not significantly increase. So, we select 1.5 equiv of K_2CO_3 as base to promote the coupling reaction between aryl halides and terminal alkynes. As for why the strong base (NaOH and KOH) can not effectively promote the transformation reaction, it is not fully clear at present and further work on this is underway.

Structure Characterization of Sonogashira reaction products (1a-1l):

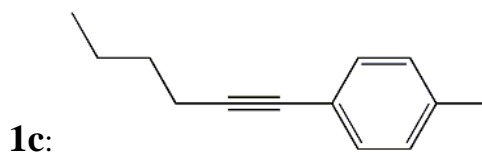
The 1H NMR, FT-IR and MS data as well as the melting point (m.p.) of the catalytic reaction products (1a-1l) is given as follows.



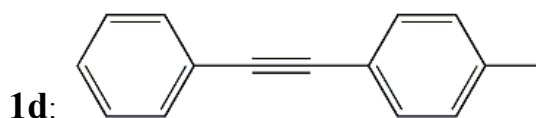
Light yellow liquid product. 1H NMR δ (400 MHz, $CDCl_3$): 7.09–7.26 (m, 4H), 2.44 (t, $J=7.0$ Hz, 2H), 2.33 (s, 3H), 1.49–1.64 (m, 4H), 0.99 (t, $J=7.0$ Hz, 3H). FT-IR (KBr): ν 3028, 2958, 2216, 1620, $1534cm^{-1}$. MS: m/z (%): 172 (10, M^+), 157 (100), 143 (52), 142 (32), 129(45), 115(17).



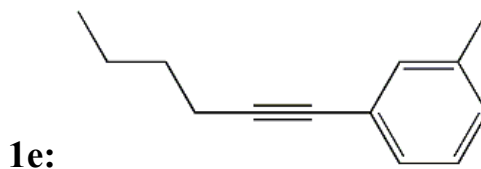
Light yellow solid product. m.p.: $60^\circ C$. 1H NMR δ (400 MHz, $CDCl_3$): 7.52–7.54 (m, 4H), 7.25–7.37 (m, 6H). FT-IR (KBr): ν 3022, 1628, $1545 cm^{-1}$. MS: m/z (%): 179 (22, M^+), 178 (100, M^+).



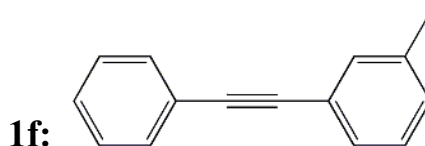
Light yellow liquid product. 1H NMR δ (400 MHz, $CDCl_3$): 7.26 (d, $J=8.4$ Hz, 2H), 7.09 (d, $J=8.4$, 2H), 2.38 (t, $J=7.2$ Hz, 2H), 2.31 (s, 3H), 1.47–1.57 (m, 4H), 0.94 (t, $J=7.2$ Hz, 3H). FT-IR (KBr): ν 3022, 2945, 2210, 1625, $1528cm^{-1}$.



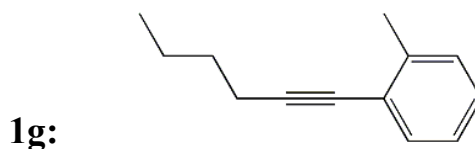
Light yellow solid product. **m.p.:** 70°C. **¹H NMR** δ (400 MHz, CDCl₃): 7.53–7.56 (m, 2H), 7.45 (d, $J=8.0$ Hz, 2H), 7.35–7.38 (m, 3H), 7.18 (d, $J=8.0$ Hz, 2H), 2.39 (s, 3H). **FT-IR** (KBr): ν 3016, 2237, 1634, 1543 cm⁻¹. **MS:** m/z (%): 192 (100, M⁺), 191 (45), 165 (10), 115 (4).



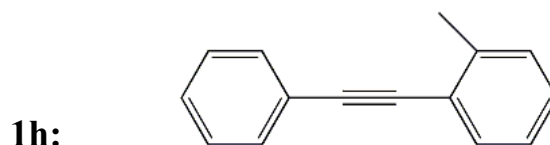
Light yellow liquid product. **¹H NMR** δ (400 MHz, CDCl₃): 7.09–7.26 (m, 4H), 2.44 (t, $J=7.0$ Hz, 2H), 2.33 (s, 3H), 1.49–1.64 (m, 4H), 0.99 (t, $J=7.0$ Hz, 3H). **FT-IR** (KBr): ν 3028, 2958, 2216, 1620, 1534cm⁻¹. **MS:** m/z (%): 172 (10, M⁺), 157 (100), 143 (52), 142 (32), 129(45), 115(17).



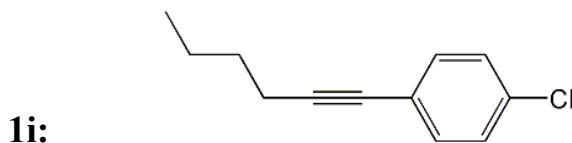
Light yellow liquid product. **¹H NMR** δ (400 MHz, CDCl₃): 7.57–7.59 (m, 2H), 7.38–7.42 (m, 5H), 7.27–7.30 (m, 1H), 7.19 (d, $J=8.0$ Hz, 1H), 2.40 (s, 3H). **FT-IR** (KBr): ν 3014, 2228, 1645, 1553 cm⁻¹. **MS:** m/z (%): 192 (100, M⁺), 191 (48), 165 (12), 115 (6).



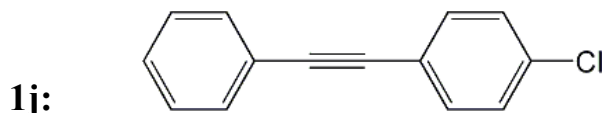
Light yellow liquid product. **¹H NMR** δ (400 MHz, CDCl₃): 7.39 (d, $J=7.4$ Hz, 1H), 7.12–7.20 (m, 3H), 2.48 (t, $J=7.0$ Hz, 2H), 2.44 (s, 3H), 1.52–1.66 (m, 4H), 0.98 (t, $J=7.0$ Hz, 3H). **FT-IR** (KBr): ν 3042, 2962, 2225, 1631, 1543cm⁻¹. **MS:** m/z (%): 172 (31, M⁺), 157 (100), 144 (30), 143 (86), 142 (48), 130 (31), 128 (60), 127 (39), 115(25).



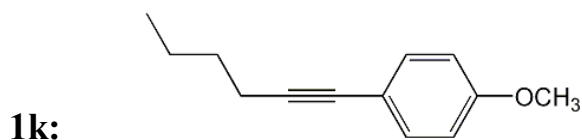
Light yellow liquid product. $^1\text{H NMR}$ δ (400 MHz, CDCl_3): 7.56–7.61 (m, 3H), 7.38–7.42 (m, 3H), 7.22–7.28 (m, 3H), 2.57 (s, 3H). **FT-IR** (KBr): ν 3025, 2218, 1625, 1530cm^{-1} . **MS**: m/z (%): 192 (100, M^+), 191 (44), 165 (11), 115 (7).



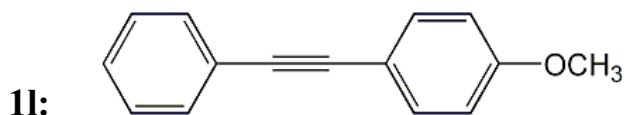
Light yellow liquid product. $^1\text{H NMR}$ δ (400 MHz, CDCl_3): 7.33 (d, $J=8.4\text{Hz}$, 2H), 7.26 (d, $J=8.4\text{Hz}$, 2H), 2.41 (t, $J=7.2\text{Hz}$, 2H), 1.47–1.61 (m, 4H), 0.96 (t, $J=7.2\text{Hz}$, 3H). **FT-IR** (KBr): ν 3045, 2968, 2234, 1630, 1554cm^{-1} . **MS**: m/z (%): 193 (8, M^++1), 192 (15, M^++1), 191 (15, M^+), 179 (34), 177 (100), 163 (67), 157 (59), 149 (73), 142 (60), 141 (42), 129 (47), 127 (29), 115 (46), 114 (38), 113 (27).



Light yellow liquid product. **m.p.**: 82°C . $^1\text{H NMR}$ δ (400 MHz, CDCl_3): 7.45–7.54 (m, 4H), 7.32–7.36 (m, 5H). **FT-IR** (KBr): ν 3042, 2220, 1626, 1524cm^{-1} . **MS**: m/z (%): 214 (100, M^++1), 212 (44), 176 (14), 152 (3).



Light yellow oil-like product. $^1\text{H NMR}$ (400 MHz, CDCl_3): δ 0.89 (t, $J = 6.8\text{ Hz}$, 3H), 1.34 - 1.41 (m, 2H), 1.43 - 1.55 (m, 2H), 2.32 (t, $J = 6.8\text{ Hz}$, 2H), 3.73 (s), 6.74 (d, $J = 8.4\text{ Hz}$, 2H), 7.24 (d, $J = 8.4\text{ Hz}$, 2H). **FT-IR** (neat): ν 3012, 2957, 2134, 1596, 1493, 1120, 1027 cm^{-1} . **MS**: m/z (%) 188 (100, M^+), 173 (43), 159 (60), 145 (80), 102 (31).



Light yellow solid product. **m.p.**: 60°C . $^1\text{H NMR}$ (400 MHz, CDCl_3): δ 3.86 (s, 3H), 6.91 (d, $J = 8.5\text{ Hz}$, 2H), 7.33 - 7.39 (m, 3H), 7.50 - 7.56 (m, 4H). **FT-IR** (KBr): ν 3021, 1602, 1521, 1108 cm^{-1} . **MS**: m/z (%) 208 (100, M^+), 193 (38), 165 (27).

Characterization of the Isolated Catalyst after Completion of Catalytic Reaction:

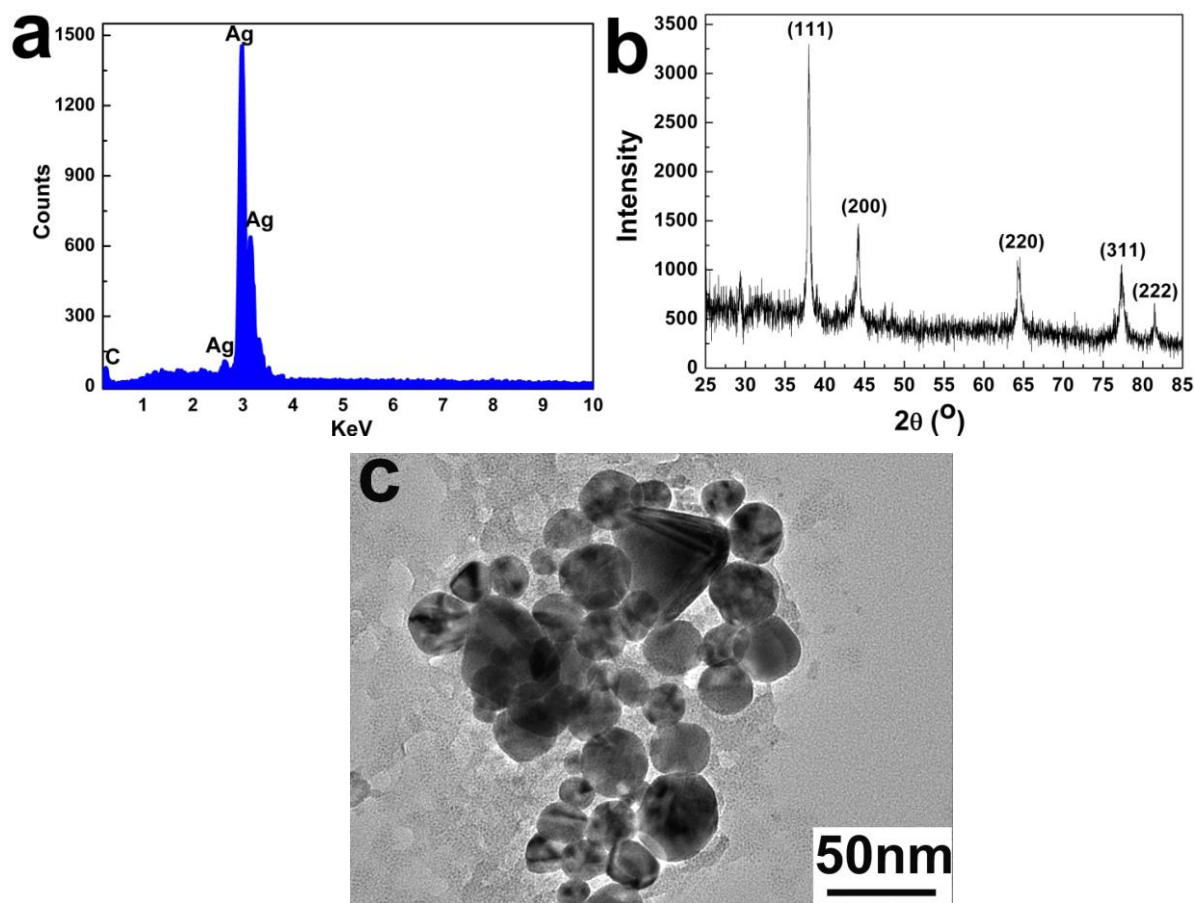


Figure S3 The characterization of the isolated catalyst from the organic layer after completion of the third catalytic recycle. (a) EDX pattern. (b) XRD pattern. (c) TEM image.

Leaching and Control Experiments

We select the coupling reaction of *p*-iodotoluene with phenylacetylene as the model reaction and do the leaching experiments repeatedly. The detailed processes are as follows: when the reaction is performed at 80 °C for 54 min, the reactor is immediately transferred into ice-water bath to quench the reaction. Subsequently, the solid catalysts are removed by centrifugation at 13000 rpm for 15 min and the supernatant liquid is preserved. Then, the co-catalysts and base are added to the supernatant liquid and kept at the same reaction condition for another 66 min. Under this case, the isolated yield is about 59%. Before separating the solid catalysts (reacting at 80 °C for 54 min), the control experiment shows that the yield is 50 %. It implies that the yield is only raised ~9 % after removing the solid catalysts and reacting for another 66 min, which is much lower than that containing the

solid catalysts in the same reaction time (66 min, yield rising ~ 44%). ICP analysis reveals that there is about 2.04 % of Ag leaching into the supernatant liquid, which may be reason for the yield rising about 9% after removing the solid catalysts. Usually, we may think that the leached Ag exists as a $\text{Ag}(\text{PPh}_3)\text{I}$ complex in the supernatant liquid and acts as the real catalyst. In order to learn the related information, we directly use $\text{Ag}(\text{PPh}_3)\text{I}$ complex as the catalyst and do the control experiment under the same reaction conditions. The results demonstrate that nearly no objective product can be detected even if the reaction time is extended to 3 h, indicating that the $\text{Ag}(\text{PPh}_3)\text{I}$ complex can't catalyze the cross-coupling reaction under our experimental conditions. Based on those experimental results, the real catalyst should be Ag NCs.

Synthesis and Characterization of Pd NCs: The synthetic procedure is similar to that of Ag NCs. The only difference is that using solid $\text{Pd}(\text{CH}_3\text{COO})_2$ instead of solid AgNO_3 . The post-treatment process is the same as that for Ag NCs. Corresponding TEM, HRTEM and XRD results of the synthesized Pd NCs are shown in **Fig. S4**. From Fig. S4a, nearly monodisperse and branched Pd NCs can be observed. The diameter of each branch is about 4-6 nm. The HRTEM analysis (shown in the inset of Fig. S4a) gives clear lattice fringes. The lattice spacing is measured to be about 2.20 Å, corresponding to the interplanar separation of (111) plane of *fcc* Pd. The XRD results (Fig. S4b) further confirm that the obtained product is *fcc* Pd, which is consistent with HRTEM analysis.

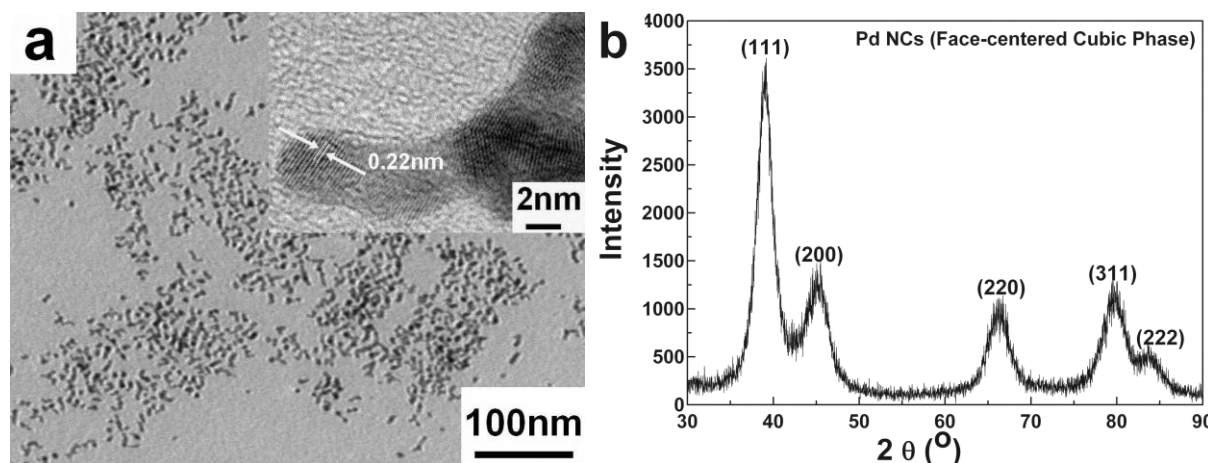


Figure S4 (a) The TEM image of the synthesized Pd NCs. The inset shows the corresponding HRTEM image of an individual Pd NC. (b) The XRD pattern of the obtained Pd NCs.

Catalytic Dynamic Experiments

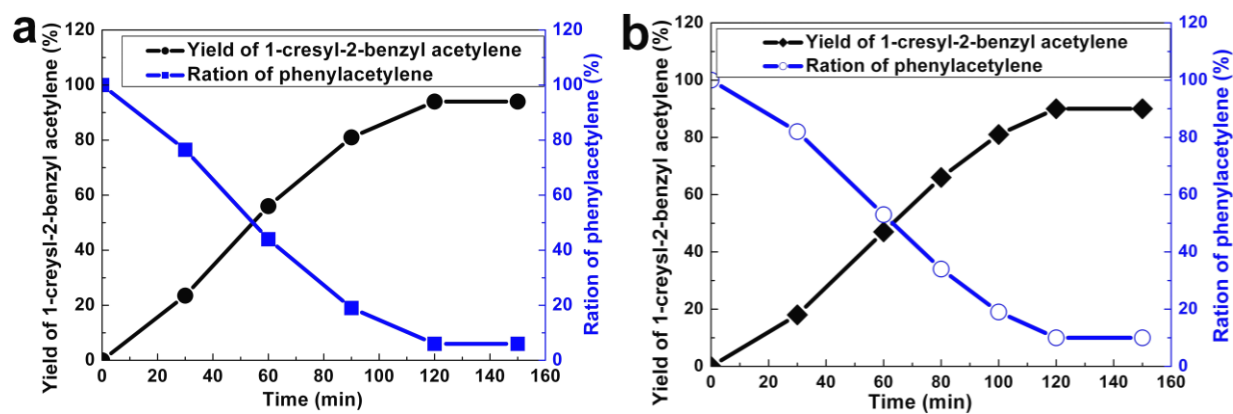


Figure S5 The catalytic dynamic plots of (a) 6 nm Ag NCs and (b) Pd NCs for catalyzing the coupling between phenylacetylene and *p*-isotoluene at 80°C.